FINITE ELEMENT MODEL REDUCTION FOR ROTATING SYSTEMS

Andrea Argondizza
Applied Mechatronic Engineering & Technologies S.r.l.
Via San Luigi 20, 10043 Orbassano (Torino), Italy

S. Carabelli, A. Tonoli
Mechatronics Laboratory, Politecnico di Torino
Corso Duca degli Abruzzi 24, 10129 Torino, Italy

INTRODUCTION

Complex rotors are usually modeled by means of Finite Element Method (FEM) to cope with nonelementary shape of the shaft and of the rotating appendices connected to it (figure 1). To account for the the complex geometry, the discretization at the base of the FEM model is usually characterized by a high number of nodes and, correspondingly of degrees of freedom. The FE model is then characterized by a high number of densely populated modes. Such an high order model takes the geometrical complexity of the structure into account but may fail to bring into evidence the more relevant modes both in terms of energy content and observability and controllability by available sensors and actuators. Nevertheless, FE high order models may indicate substantial criticities in the design of complex rotors due to unwanted parasitic resonances in the working frequency range of the machine.

In any case, modern rotor engineering strongly relies on FE numerical models before undertaking any actual construction. In particular for what the active magnetic bearings (AMB) are concerned, a model is necessary to design the control law to stabilize the system represented by the rotor and the active magnetic suspensions. In such a context, only a few modes are really relevant to the system stability but they must be identified within their densely populated frequency range. In other words, resonant modes due to appendices supported by the rotor must be separated from those due to the rotor itself once they are checked to be of minor importance (energetically speaking).

From the above reported considerations, when dealing with FE models the following needs emerge:

- some physically sound and numerically robust model reduction techniques and
- some reliable selection techniques to choose the modes to be kept into account in the reduced model.

The former need is here addressed by means of a modal transformation directly based on the dynamic equation in the so-called configuration space. The proposed procedure relies on the exploitation of the symmetric and asymmetric structure of the system matrices typical of a gyroscopic system. The equations of the motion are transformed in a decoupled modal state space that takes the gyroscopic terms into account [2]. The effect of a reduction by truncation or residualization is then studied in the decoupled modal state space and it leads to a reduction technique by truncation that keeps the static gain (usually obtained only with a residualization procedure of reduction).

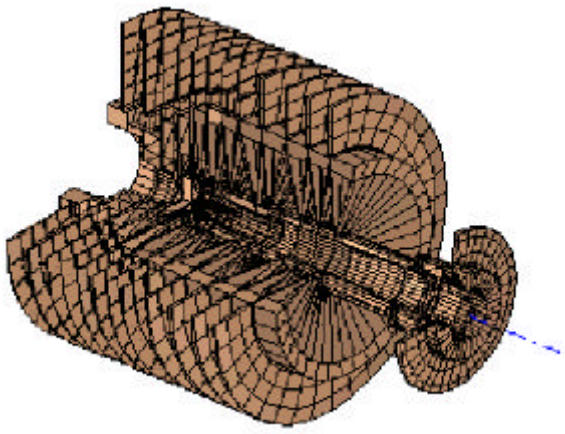

Figure 1: Finite element model meshing of a typical turbomolecular pump rotor on active magnetic bearings.

The latter need is achieved by means of a modal cost approach that accounts for the so-called mechanical energy (kinetic and potential) of the system. In order to check its numerical reliability, it has been compared with a physical approach which consists in decreasing the material density and Young's modulus of parts of the rotor while preserving their ratio. This method makes the influence of these substructures on the main rotor to vanish progressively (thus effecting its natural frequencies) while maintaining their natural frequency (vanishing modes).

FE MODEL STRUCTURE

By construction, FE models are usually characterized by a considerable amount of degrees of freedom not strictly needed either for analysis or for design purposes. With the standard distinction between master and slave degrees of freedom, a first "a priori" reduction (for instance the so-called Guyan reduction) is usually carried on. For example, all rotations are usually considered slave degrees of freedom except for nodes where highly gyroscopic elements as disks are located. The resulting model yields exact results for static problems, i.e. the same results that would be obtained from the complete model.

Since the flexural, axial and torsional dynamics of a rotor may often considered uncoupled [1], only the former will be here considered, whose complete dynamical equation is the following:

$$\begin{aligned} & \mathbf{M}_{flx}\ddot{\mathbf{q}}(t) + \\ & \left[\mathbf{C}_r + \mathbf{C}_n - i\omega\mathbf{G}_{flx}\right]\dot{\mathbf{q}}(t) + \\ & \left[\mathbf{K}_{flx} - i\omega\mathbf{C}_r + \omega^2\left(\mathbf{K}_\omega + \mathbf{K}'_\omega\right)\right]\mathbf{q}(t) \\ = \; & \mathbf{f}(t) + \omega^2 e^{i\omega t}\mathbf{f}_{unb} \end{aligned} \tag{1}$$

where

$\mathbf{M}_{flx}$	Flexural mass
$\mathbf{C}_r$	Rotating damping
$\mathbf{C}_n$	Nonrotating damping
$\mathbf{G}_{flx}$	Gyroscopic effect
$\mathbf{K}_{flx}$	Flexural stiffness
$\mathbf{K}_\omega + \mathbf{K}'_\omega$	Speed dependent stiffness
ω	Spin speed
$\mathbf{q}(t) = \mathbf{x}(t) + i\mathbf{y}(t)$	Complex radial coordinates
$\mathbf{f}(t)$	External nodal forces
$\mathbf{f}_{unb}$	Static unbalances

The adoption of complex radial coordinates is expedient in rotordynamics to describe in a compact and immediate form the whirl motion as well as its forward or backward nature (differently linked to overall stability under rotation). In the case of axis symmetry complex co-ordinates allow to exploit the intrinsic decoupling of the system in two identical subsystems lying orthogonal planes. In order to work in real coordinates the following transformation is to be accomplished:

$$\mathbf{q}(t) = \mathbf{x}(t) + i\mathbf{y}(t) \longrightarrow \left\{ \begin{matrix} \mathbf{x}(t) \\ \mathbf{y}(t) \end{matrix} \right\} = \mathbf{q}(t) \tag{2}$$

that applied to equation 1 split to real and imaginary parts leads to

$$\begin{aligned} & \mathbf{M}_{flx}\ddot{\mathbf{x}}(t) + \\ & \left[\mathbf{C}_r + \mathbf{C}_n\right]\dot{\mathbf{x}}(t) + \omega\mathbf{G}_{flx}\dot{\mathbf{y}}(t) + \\ & \left[\mathbf{K}_{flx} + \omega^2\left(\mathbf{K}_\omega + \mathbf{K}'_\omega\right)\right]\mathbf{x}(t) + \omega\mathbf{C}_r\mathbf{y}(t) \\ = \; & \mathbf{f}_x(t) + \omega^2\sin(\omega t)\mathbf{f}_{unb} \end{aligned} \tag{3}$$

$$\begin{aligned} & \mathbf{M}_{flx}\ddot{\mathbf{y}}(t) + \\ & \left[\mathbf{C}_r + \mathbf{C}_n\right]\dot{\mathbf{y}}(t) - \omega\mathbf{G}_{flx}\dot{\mathbf{x}}(t) + \\ & \left[\mathbf{K}_{flx} + \omega^2\left(\mathbf{K}_\omega + \mathbf{K}'_\omega\right)\right]\mathbf{y}(t) - \omega\mathbf{C}_r\mathbf{x}(t) \\ = \; & \mathbf{f}_y(t) + \omega^2\cos(\omega t)\mathbf{f}_{unb} \end{aligned} \tag{4}$$

and, in matricial form,

$$\begin{aligned} & \mathbf{M}\ddot{\mathbf{q}}(t) + \left[\mathbf{L} + \mathbf{G}\right]\dot{\mathbf{q}}(t) + \left[\mathbf{K} + \mathbf{H}\right]\mathbf{q}(t) \\ = \; & \mathbf{f}(t) + \omega^2\mathbf{U}\mathbf{f}_{unb} \end{aligned} \tag{5}$$

where the following matrices

$$\mathbf{M} = \begin{bmatrix} \mathbf{M}_{flx} & \\ & \mathbf{M}_{flx} \end{bmatrix};\ \mathbf{G} = \begin{bmatrix} & \omega\mathbf{G}_{flx} \\ -\omega\mathbf{G}_{flx} & \end{bmatrix}$$

$$\mathbf{K} = \begin{bmatrix} \mathbf{K}_{flx} + \omega^2\left(\mathbf{K}_\omega + \mathbf{K}'_\omega\right) & \\ & \mathbf{K}_{flx} + \omega^2\left(\mathbf{K}_\omega + \mathbf{K}'_\omega\right) \end{bmatrix}$$

$$\mathbf{L} = \begin{bmatrix} \mathbf{C}_r + \mathbf{C}_n & \\ & \mathbf{C}_r + \mathbf{C}_n \end{bmatrix};\ \mathbf{H} = \begin{bmatrix} & \omega\mathbf{C}_r \\ -\omega\mathbf{C}_r & \end{bmatrix}$$

clearly show their symmetric and antisymmetric structure. For what the the size of the system of equation 5 is concerned, the adoption of real coordinates doubles the order of the system. If n is the number of degrees of freedom in complex coordinates, the number of degrees of freedom in real co-ordinates is $2n$ and the square matrices M, L, G, K, H are of order $2n \times 2n$.

Modal model via direct Cholesky transformation

The equations of the motion of a general linear gyroscopic system can be written in terms of modal co-ordinates $\boldsymbol{\xi}$ using the eigenvectors ϕ_i of the undamped and nongyroscopic system as a base for the nodal displacements.

$$\mathbf{q}(t) = \boldsymbol{\phi}\boldsymbol{\xi}(t). \tag{6}$$

The columns of the square matrix $\boldsymbol{\phi}$ are the mode shapes of the undamped and nongyroscopic system,

i.e. the eigenvectors of matrix $\mathbf{M}^{-1}\mathbf{K}$ and $\boldsymbol{\xi}$ are the modal co-ordinates. Even in the case the viscous damping matrix $\mathbf{L}$ and and the circulatory matrix $\mathbf{H}$ are null, the presence of the gyroscopic matrix $\mathbf{G}$ couples the resulting equations of the motion in the modal space. In the case of rotors with a small gyroscopic effect the coupling between the various modes can be neglected and the procedure allows to obtain a set of decoupled equations in the configuration space. In the case of highly gyroscopic rotors such as those shown in figure 1 the coupling terms can not be neglected. Even if he use of modal co-ordinates does not allow to obtain a decoupling, it is adopted as it allows a more straightforward tuning of natural frequencies and dampings by comparison with the experimental measurements. To be noted that this approach can be adopted to the equations of the motion in complex co-ordinates (equation 1).

The decoupling of the dynamic equations can be dealt with in a more systematic way if the equations of the motion of the system are expressed in a state space form. The most commonly adopted alternative in this case is to rewrite equation 5 as a general linear dynamical system.

$$\begin{aligned} \dot{\mathbf{x}} &= \mathbf{A}\mathbf{x} + \mathbf{B}\mathbf{u} \\ \mathbf{y} &= \mathbf{C}\mathbf{x} \end{aligned} \tag{7}$$

where the state and external input vectors $\mathbf{x}$ and $\mathbf{u}$ are

$$\mathbf{x} = \{\mathbf{q}, \dot{\mathbf{q}}\}^T; \quad \mathbf{u} = \mathbf{f}$$

The dependance from the time t of has been dropped for simplicity. Matrices $\mathbf{A}$, $\mathbf{B}$, $\mathbf{C}$ are

$$\begin{aligned} \mathbf{A} &= \begin{bmatrix} \mathbf{0} & \mathbf{I} \\ -\mathbf{M}^{-1}(\mathbf{K}+\mathbf{H}) & -\mathbf{M}^{-1}(\mathbf{G}+\mathbf{L}) \end{bmatrix} \\ \mathbf{C} &= \begin{bmatrix} \mathbf{T}_{out} & \mathbf{0} \end{bmatrix}; \quad \mathbf{B} = \begin{bmatrix} \mathbf{0} \\ \mathbf{M}^{-1}\mathbf{T}_{in} \end{bmatrix} \end{aligned}$$

the output matrix $\mathbf{C}$ has been written under the assumption that only displacement sensors are installed on the structure, matrix $\mathbf{T}_{out}$ accounts for their location and gain. The input selection matrix $\mathbf{T}_{in}$ accounts for the location of the forces acting on the structure.

The state equations in physical co-ordinates 7 can be decoupled using a Jordan canonical form. It is worth to point out that the generality of the method allows to obtain a decoupled set of equations even in the case of a heavily damped system. By converse the generality of the method does not allow to exploit the symmetries and anti-symmetries peculiar of a gyroscopic system.

As already pointed out, the complex geometry of most rotors of practical relevance, the number of nodes needed for their FEM discretization can be very high. The order of the matrices involved in equation 5 is then high and they are usually characterized by high modal density. The high modal density and the size of the matrices makes the computation of a canonical form of equation 7 a numerically ill conditioned problem.

An alternative solution to decouple the equations of motion of a gyroscopic system has been proposed by Meirovitch [2] in the case the viscous damping $\mathbf{L}$ and the circulatory matrix $\mathbf{H}$ are null.

The assumption that the system is undamped is justified by the usually small dissipation affecting the rotor and its supports. This assumption can fail in the case of rotors supported magnetic bearings where the presence of a high damping due to the magnetic supports can lead to a significant coupling between the modes. The equations of the motion 5 can be rewritten in a state space form using the same state vector adopted in equations 7

$$\mathbf{M}^*\dot{\mathbf{x}} + \mathbf{G}^*\mathbf{x} = \mathbf{T}^*\mathbf{f} \tag{8}$$

where matrices $\mathbf{M}^*$ and $\mathbf{G}^*$ and $\mathbf{T}^*$ are obtained from the mass, the stiffness the gyroscopic and the input matrices as

$$\mathbf{M}^* = \begin{bmatrix} \mathbf{K} & \mathbf{0} \\ \mathbf{0} & \mathbf{M} \end{bmatrix}; \; \mathbf{G}^* = \begin{bmatrix} \mathbf{0} & -\mathbf{K} \\ \mathbf{K} & \mathbf{G} \end{bmatrix}; \; \mathbf{T}^* = \begin{bmatrix} \mathbf{0} \\ \mathbf{T}_{in} \end{bmatrix}$$

The state form of equation 8 takes advantage of peculiar characteristics of matrices $\mathbf{K}$, $\mathbf{M}$, and $\mathbf{G}$ such as:

- the mass matrix $\mathbf{M}$ is real, symmetric and positive semi-definite, matrix $\mathbf{M}$ fails to be positive definite only when nodes with no associated mass are included in the finite element model;
- the stiffness matrix $\mathbf{K}$ is real, symmetric and usually positive semi-definite, matrix $\mathbf{K}$ fails to be strictly positive definite in the case of unsupported rotors. In the case of rotors supported by magnetic bearings the intrinsic negative stiffness of the magnetic actuators makes matrix $\mathbf{K}$ negative-definite
- the gyroscopic matrix $\mathbf{G}$ is anti-symmetric ($\mathbf{G}^T = -\mathbf{G}$).

>From the properties of matrices $\mathbf{K}$ $\mathbf{M}$ and $\mathbf{G}$ it follows that the state matrices $\mathbf{M}^*$ and $\mathbf{G}^*$ are symmetric and anti-symmetric respectively.

Under the assumption that:

- the nodes with no associated mass are not included in the FEM model, and
- the rotor is supported by springs with positive stiffness,

matrix $\mathbf{M}^*$ becomes symmetric and positive-definite and a Cholesky decomposition can be applied to it.

$$\mathbf{M}^* = \mathbf{L}\mathbf{L}^T \tag{9}$$

where $\mathbf{L}$ is a lower triangular nonsingular real matrix. In the case of rotors supported by magnetic bearings the assumption that the rotor is supported by springs with positive stiffness is equivalent to assume that the feedback control is able to drive the magnetic actuators with a proportional gain high enough to compensate for their intrinsic negative stiffness.

Taking the Cholesky decomposition 9 into account, the state equations 8 can then be rewritten in a state space modal form as

$$\dot{\boldsymbol{\xi}} = \quad \boldsymbol{\xi} + \Psi\mathbf{f}. \tag{10}$$

The modal state and input matrices and Ψ are given by

$$= -\Gamma^T\tilde{\mathbf{G}}\Gamma; \qquad \Psi = \Gamma^T\mathbf{L}^{-1}\mathbf{T}^* \tag{11}$$

where matrix $\tilde{\mathbf{G}}$ is obtained from matrix $\mathbf{G}^*$ with the following linear transformation

$$\tilde{\mathbf{G}} = \mathbf{L}^{-1}\mathbf{G}^*\mathbf{L}^{-T} = -\tilde{\mathbf{G}}^T \tag{12}$$

and the columns of matrix Γ are the eigenvectors of the matrix Φ

$$\Phi = \tilde{\mathbf{G}}^T\tilde{\mathbf{G}}. \tag{13}$$

Due to the antisymmetry of matrix $\tilde{\mathbf{G}}$ (equation 12), matrix Φ is characterized by a set of $2n$ real and positive eigenvalues λ_i with multiplicity 2 each. Furthermore, the 2 eigenvectors Λ_i and Θ_i corresponding to each eigenvalue λ_i are orthogonal. They can be included as columns of two matrices Λ and Θ of order $4n \times 2n$ such that

$$\Gamma = \begin{bmatrix} \Lambda & \Theta \end{bmatrix} \tag{14}$$

The transformation between modal states $\boldsymbol{\xi}$ and physical states $\mathbf{x}$ is then

$$\mathbf{x} = \mathbf{L}^{-T}\Gamma\boldsymbol{\xi} = \mathbf{L}^{-T}\begin{bmatrix} \Lambda & \Theta \end{bmatrix}\begin{Bmatrix} \boldsymbol{\eta} \\ \boldsymbol{\zeta} \end{Bmatrix}. \tag{15}$$

Modal states $\boldsymbol{\eta}$ and $\boldsymbol{\zeta}$ correspond to the mode shapes included in the two orthogonal sets Λ and Θ.

Due to the properties of matrices Γ and $\tilde{\mathbf{G}}$, the modal state matrix is antisymmetric and it can be split in a 2 diagonal form

$$= -\begin{bmatrix} \mathbf{0} & \boldsymbol{\omega} \\ -\boldsymbol{\omega}^T & \mathbf{0} \end{bmatrix} \tag{16}$$

matrix $\boldsymbol{\omega}$ $(2n \times 2n)$ is diagonal, its elements are the natural frequencies of the system. The bi-diagonal and anti-symmetric structure of matrix allows to split the state equations 10 in $2n$ couples of equations of the type

$$\left.\begin{aligned} \dot{\eta}_i &= -\omega_i\zeta_i + f_{\eta i} \\ \dot{\zeta}_i &= \omega_i\eta_i + f_{\zeta i} \end{aligned}\right\} \quad i = 1, \ldots, 2n \quad \omega_i = \sqrt{\lambda_i}. \tag{17}$$

each couple of equations is decoupled from the all the other.

MODAL COST

Modal cost analysis [3], [4] may be considered as a mean to obtain a measure of the relative importance of each mode, it relies on an underlying set of reference input and initial conditions. In the case of unitary impulse excitation and null initial conditions, the overall modal cost may be written as

$$V = \sum_{i=1}^{n} V_i = \sum_{i=1}^{n} \int_0^\infty \boldsymbol{\xi}_i(t)^T \mathbf{W}_v \boldsymbol{\xi}_i(t)\, dt \tag{18}$$

where $\mathbf{W}_v$ is a weighing matrix. In the case of a mechanical system if $\mathbf{W}_v = \mathrm{diag}(\mathbf{M}, \mathbf{K})$ the term V_i is related to the mechanical energy (kinetic+elastic energy) associated with the ith modal state $\boldsymbol{\xi}_i$.

The modal cost is computed as

$$V = tr\{\mathbf{W}_v\mathbf{X}\} \tag{19}$$

where $\mathbf{X}$ satisfies the Lyapunov equation:

$$\mathbf{X}^T + \mathbf{X} + \boldsymbol{\psi}\boldsymbol{\psi}^T = 0 \tag{20}$$

where matrices and $\boldsymbol{\psi}$ are obtained from equation 11.

Vanishing modes

In order to check the results offered by modal cost computation, a completely different approach to identify the relevant modes is here proposed. It relies on assembling many finite element models that differ only for a parameter γ that premultiply both the material density and the Young's modulus of the appendices substructures, thus leaving unchanged their natural frequency but making their influence on the

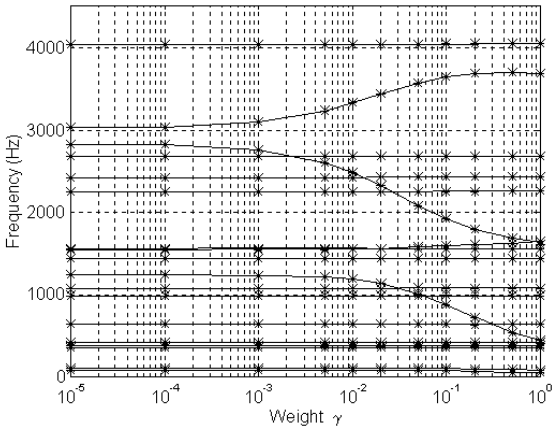

Figure 2: Modal natural frequencies as a function of γ parameter.

main structure to "vanish". The vanished appendices no longer effect inertially the main structure whose natural frequency turns out to change with parameter γ . The method has been adopted to investigate the importance of the local modes of the discs and the array of blades for the rotor of figure 1. Figure 2 shows the undamped natural frequencies of the rotor as a function of the weighting parameter γ. The few modes influenced by the vanishing of parameter γ are the modes of the shaft that are affected by the inertial behaviour of the appendices as rigid bodies.Table reports the comparison between modal costs computed for the same rotor and the results yielded by the vanishing modes computation. The natural frequencies for $\gamma = 10^{-5}$ and $\gamma = 1$ are reported in the second and fourth columns. The modal costs computed for $\gamma = 1$ are reported in column 5. Local modes of the substructure are not substantially affected by vanishing of their mass, they are then in the same row of the table. The blanks at the left of mode #6 at $\gamma = 1$ because this mode becomes mode #9 at $\gamma = 10^{-5}$, this is then a mode of the shaft which is affected by the appendices. The migration of this mode is also shown in figure 2. Similarly mode #16 at $\gamma = 1$ becomes mode #19 at $\gamma = 10^{-5}$.

The modal costs reported in the last column of table show high values for modes #1 and #2 (rigid body modes) and for the modes which show substantial changes in the "vanishing" process. The values of the modal cost show that modal costs may fail to provide clear indication in the case of very close modes.

(#)	Freq. (Hz)	(#)	Freq. (Hz)	Cost (%)
$\gamma = 10^{-5}$		$\gamma = 1$		
1	69.7	1	51.5	85.7
2	148.0	2	84.6	11.3
3	353.7	3	353.6	0.06
4	383.0	4	380.8	0.10
5	426.0	5	418.6	0.86
		6	448.6	0.62
6	641.7	7	645.6	$2.1{\cdot}10^{-3}$
7	994.0	8	996.3	$1.8{\cdot}10^{-3}$
8	1067.4	9	1071.8	$1.0{\cdot}10^{-3}$
9	1236.5			
10	1433.8	10	1433.9	$3{\cdot}10^{-6}$
11	1433.9	11	1438.3	$2{\cdot}10^{-3}$
12	1545.3	12	1554.0	$3{\cdot}10^{-5}$
13	1554.1	13	1554.1	$2{\cdot}10^{-6}$
14	1554.1	14	1554.1	$3{\cdot}10^{-8}$
15	1554.1	15	1611.8	$2.4{\cdot}10^{-2}$
		16	1644.8	$6.6{\cdot}10^{-2}$
16	2246.0	17	2251.5	$3{\cdot}10^{-4}$
17	2420.7	18	2425.8	$3{\cdot}10^{-4}$
18	2678.6	19	2681.5	$2{\cdot}10^{-3}$
19	2830.0			
20	3033.5	20	3685.7	$4{\cdot}10^{-4}$
21	4042.6	21	4046.9	$3{\cdot}10^{-2}$

Table 1: Modal costs computed in the extreme cases of structure with real and vanished modes, respectively $\gamma = 1$ and $\gamma = 10^{-5}$. Note the different order number due to migration of the shaft modes.

MODAL REDUCTION

The decoupling of the modal state space equation 10 can be exploited in order to reduce the order of the model. The number of degrees of freedom of the finite element model is, in fact, largely determined by geometric complexity of the rotor. To reduce the number of degrees of freedom of equation 8 including the dynamic behavior relevant for the point of the control design the modal co-ordinates can be split in a master and in a slave subset. Usually these two subsets is performed on a frequency basis, in the following the selection is performed using a criteria based on a "vanishing modes" analysis.

Equation 17 show that the modal state equations 10 are organized in couples with an anti-symmetric state matrix. The selection between master and the slave subset must then be made considering each couple of modal variables as if it were an undivisible entity. Under the assumption that the response of the modes included in the slave subset is

static the state equations 10 become:

$$\dot{\boldsymbol{\xi}}_m + \quad {}_m\boldsymbol{\xi}_m \quad = \quad \Psi_m \mathbf{f} \tag{21}$$

$$\quad {}_s\boldsymbol{\xi}_s \quad = \quad \Psi_s \mathbf{f} \tag{22}$$

where

$$\Psi_m = \Gamma_m^T \mathbf{L}^{-1} \mathbf{T}^*; \quad \Psi_s = \Gamma_s^T \mathbf{L}^{-1} \mathbf{T}^* \tag{23}$$

The slave states are obtained from equation 22

$$\boldsymbol{\xi}_s = \quad {}_s^{-1} \Psi_s \mathbf{f} \tag{24}$$

It can be shown that

$$\mathbf{x} = \mathbf{L}^{-T} \Gamma \boldsymbol{\xi} = \mathbf{L}^{-T} \Gamma_m \boldsymbol{\xi}_m + \mathbf{L}^{-T} \Gamma_s \quad {}_s^{-1} \Gamma_s^T \mathbf{L}^{-1} \mathbf{T}^* \mathbf{f} \tag{25}$$

Due to the orthogonality of the vectors contained in the matrix Γ and its submatrices and due to anti-symmetry of matrix ${}_s^{-1}$ the static contribution of the input force on the configuration vector $\mathbf{x}$ is null

$$\mathbf{L}^{-T} \Gamma_s \quad {}_s^{-1} \Gamma_s^T \mathbf{L}^{-1} = 0 \tag{26}$$

Truncation versus residualization

As the direct link between the state vector $\mathbf{x}$ and the input force $\mathbf{f}$ vanishes, the static response of the modes included in the slave subset does not contribute to the state vector x obtained from the reduced model. Taking the output equation 7 the static response of the slave modes do not give a contribution to the output.

Figure **??** shows the transfer function between the magnetic actuator located in the bell shaped structure of figure 1 and and the corresponding sensor. The continuous curve is relative to the complete model. The dashed one is obtained using the above described modal reduction. Only the modes shown to be important by the "vanishing modes analysis" have been included in the master mode set. The comparison shows that the reduced model preserves the same pole-zero structure of the complete model up to frequencies close to that of the last mode included in the master set.

CONCLUSIONS

A modal reduction technique based on a non standard (Jordan) modal form is presented. The modal transformation is directly based on the matricial second order representation of the dynamical equation of the undamped gyroscopic system. It is shown that this form allows a reduction by truncation that keeps the static gain and the zero-pole structure of the complete system (as for the so-called residualization reduction methods).

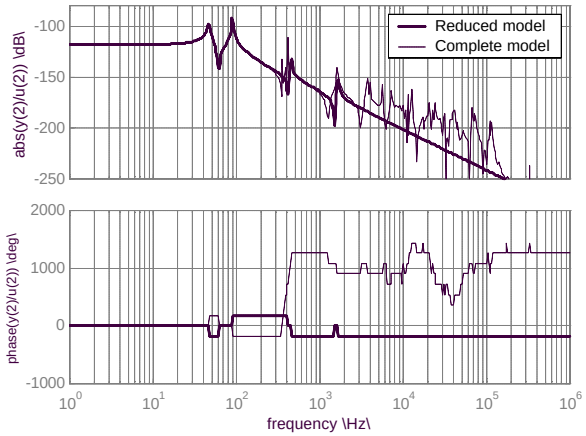

Figure 3: Force to displacement transfer function of rotor of figure 1.

In order to select the modes to be included in the reduced model, a modal cost analysis is compared to a physically based technique to show its achievable reliability. The analysis confirms that modal costs may fail to provide clear indication in the case of very close modes. The proposed "vanishing modes" technique is shown to be able to cope with these occurrences but requires extensive finite element model recomputation.

References

[1] G. Genta, *Vibration of Structures and Machines*. Springer-Verlag, 1995.

[2] L. Meirovitch, *Dynamics and Control of Structures*. John Wiley & Sons, 1990.

[3] J. Junkins and Y. Kim, *Introduction to Dynamics and Control of Flexible Structures*. AIAA Education Series, 1993.

[4] R. Skelton and P. Hughes, "Modal cost analysis for linear matrix-second-order systems," *ASME Journal of Dynamic Systems, Measurement, and Control*, vol. 102, pp. 151–158, September 1980.